NANO LETTERS

2007
Vol. 7, No. 5
1297−1303

Molecular Plasmonics with Tunable Exciton–Plasmon Coupling Strength in J-Aggregate Hybridized Au Nanorod Assemblies

Gregory A. Wurtz,* Paul R. Evans, William Hendren, Ronald Atkinson, Wayne Dickson, Robert J. Pollard, and Anatoly V. Zayats

Centre for Nanostructured Media, IRCEP, The Queen's University of Belfast, Belfast BT7 1NN, United Kingdom

William Harrison

Optical Molecular Imaging Group, Medical Science & Technology Center, Kodak Research Laboratories, Rochester, New York 14650-2102

Christopher Bower

Kodak European Research, 332 Science Park, Milton Road, Cambridge CB4 0WN, United Kingdom

Received February 5, 2007; Revised Manuscript Received March 30, 2007

ABSTRACT

Controlling coherent electromagnetic interactions in molecular systems is a problem of both fundamental interest and important applicative potential in the development of photonic and opto-electronic devices. The strength of these interactions determines both the absorption and emission properties of molecules coupled to nanostructures, effectively governing the optical properties of such a composite metamaterial. Here we report on the observation of strong coupling between a plasmon supported by an assembly of oriented gold nanorods (ANR) and a molecular exciton. We show that the coupling is easily engineered and is deterministic as both spatial and spectral overlap between the plasmonic structure and molecular aggregates are controlled. We think that these results in conjunction with the flexible geometry of the ANR are of potential significance to the development of plasmonic molecular devices.

The fabrication of nanostructures and control of their interaction in integrated device architectures represents one of the great challenges scientists are facing today. The past decade has witnessed increasing progress toward this aim primarily because of the development of fabrication and characterization tools suitable for nano-objects. One of the promising routes, of increasing interest, in the physical sciences is to make use of surface plasmon−polaritons (SPP).[1−3] These electromagnetic surface modes are associated with the coherent excitation by photons of the free electron density charge waves at the interface between a metal and a dielectric material.[4] They are extremely sensitive to the geometry of the supporting structure, thus allowing an extensive tuning of both the spectral properties and associated electromagnetic field distribution by appropriate structural design. Applications ranging from chemical sensing to surface-enhanced spectroscopies and electromagnetic energy guiding are taking advantage of these unique properties.[5−8] A further step towards implementing nanoscale-integrated optical circuitry is in designing active devices that demonstrate basic functionalities such as switching, lasing, energy storage, and conversion.[2,9,10] This can be achieved by coupling plasmonic modes to appropriately chosen active materials. Organic semiconductors materials, such as J-aggregates, are thought to offer great potential because they have the upper hand in low-cost manufacturing processes and possess attractive optical properties.[11]

J-aggregates support excitonic states, which are electrically neutral electrons/holes pairs, created by the absorption of photons. In photosynthetic processes, these states are used by plants to collect, store, and guide energy to the reaction

* Corresponding author. E-mail: g.wurtz@qub.ac.uk.

10.1021/nl070284m CCC: $37.00
Published on Web 04/25/2007

center for energy conversion and could therefore drive artificial devices on identical principles. Excitonic states also show very strong nonlinear optical behavior that could be used to produce stimulated sources of photons and transistor-like action. Experiments on colloidal solutions of Ag nanoparticles covered with J-aggregates demonstrated the possibility of using the strong scattering cross section and the enhanced field associated with surface plasmon to generate stimulated emission from J-aggregate excitons with very low excitation powers.[12] Their coupling to surface plasmons excitations appears therefore as a particularly attractive approach for creating low-powered optical devices. In addition, the coupling of J-aggregates with plasmonic structures presents genuine fundamental interest in the creation of mixed plasmon−exciton states.[13−15] These quasiparticles may be created if the energy of the excitonic mode is resonant with a plasmonic transition. Either weak or strong coupling can then be achieved depending on whether the transitions probabilities associated to the system's eigenmodes are still governed by the Fermi golden rule of the isolated systems. Tuning the coupling strength is therefore of particular interest to tailor the absorption and emission characteristics of the molecular semiconductor. Strong coupling was observed in different systems including microcavities, where the quasiparticle comprises cavity photons and a molecular exciton,[16,17] in plasmonic systems involving a surface plasmon−polariton (SPP) and a waveguide photon[18] and, more recently, between a SPP and an exciton.[13,14] The latter were observed in conventional plasmonic geometries, enabling no or little tunability and therefore offering minimal prospect for practical interests. In this paper, we report observations of the formation of hybrid plasmonic−excitonic states in assemblies of aligned gold (Au) nanorods surrounded by a shell of J-aggregates supporting a molecular excitonic transition dipole moment. The flexible geometry of the assembly of nanorods (ANR) was used to control the position of the J-aggregates in the plasmonic structure as well as the mixing of the hybrid system's eigenstates, offering a unique possibility in the designing of molecular plasmonic nanodevices with tailored optoelectronic functionalities.

The plasmonic structure under consideration is made of an assembly of aligned Au nanorods supported by a transparent substrate. The Au nanorods are electrochemically grown in a substrate-supported, porous, anodized aluminum oxide template (AAO). The substrate is a multilayered structure comprising a 1 mm thick glass slide, a 10 nm thick Ta_2O_5 base layer, and a 5 nm thick Au film acting as the working electrode for the electrochemical reaction. An aluminum (Al) film of up to 500 nm thick is then planar magnetron sputter deposited onto the electrode. This Al film is subsequently anodized to produce the porous alumina template. The geometry of the AAO template determines the rod diameter and spacing. These parameters, in addition to the rod length, can be tuned to control the optical properties of the ANR throughout the visible and near-infrared spectrum. The resulting nanorod assembly is strongly uniaxially anisotropic, with the optic axis aligned with the long axis of

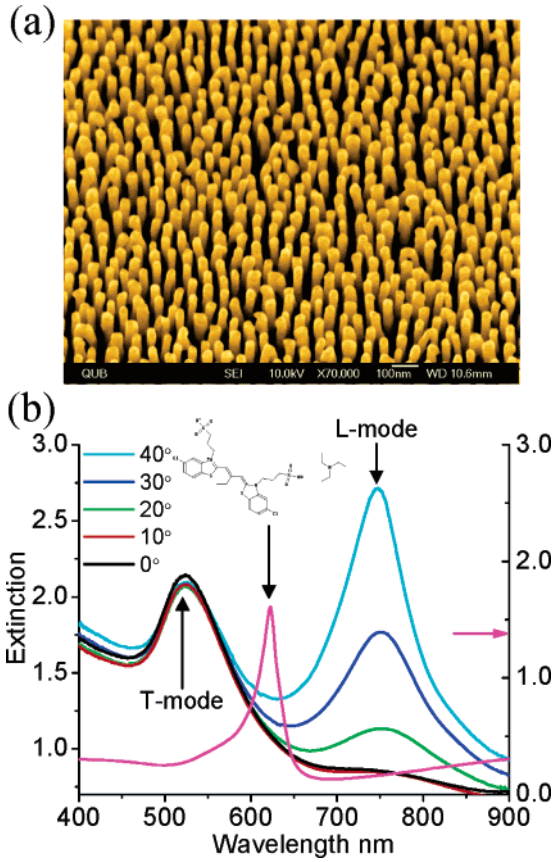

Figure 1. (a) SEM image of an assembly of Au nanorods in air. (b) Extinction spectrum of the ANR embedded in the alumina template as a function of angle of incidence. Note that the background extinction of the ANR in alumina is about 0.6. The inset shows the molecular structure of the dye used to hybridize the ANR along with its extinction spectrum shown in a magenta line when J-aggregated on a 50 nm thick smooth Au film magnetron sputtered on a glass substrate. The rod's diameter, spacing, and length are 16 nm, 50 nm, and 250 nm, respectively.

the rods oriented parallel to each other and perpendicular to the substrate. Figure 1a shows an SEM picture of a typical ANR for which the rod diameter, spacing, and length are 16, 50, and 250 nm, respectively. The extinction spectrum from such an assembly in the AAO matrix is presented in Figure 1b as a function of angle of incidence.

The spectra are dominated by two resonances whose angular dependence reflects the high degree of anisotropy in the system. The short axis of the nanorods leads to the appearance of a resonance around 500 nm that is associated to the excitation of the lowest order−dipolar−plasmon resonance of the rods. This transverse (T) resonance is addressed for electric fields polarized along the short axis and follows the behavior of a localized plasmonic mode.[19] The lower energy resonance located around 750 nm is only observed in the spectra when a component of the incident electric field is polarized along the long axis of the rods and is referred to as longitudinal (L) resonance. These resonances are regarded as eigenmodes of the structure. Both the spectral position and the angular dependence of the L-mode are reminiscent of the nature of the coupling between the rods within the assembly. In fact, the L-mode observed in Figure 1b results from the strong electromagnetic inter-rod coupling

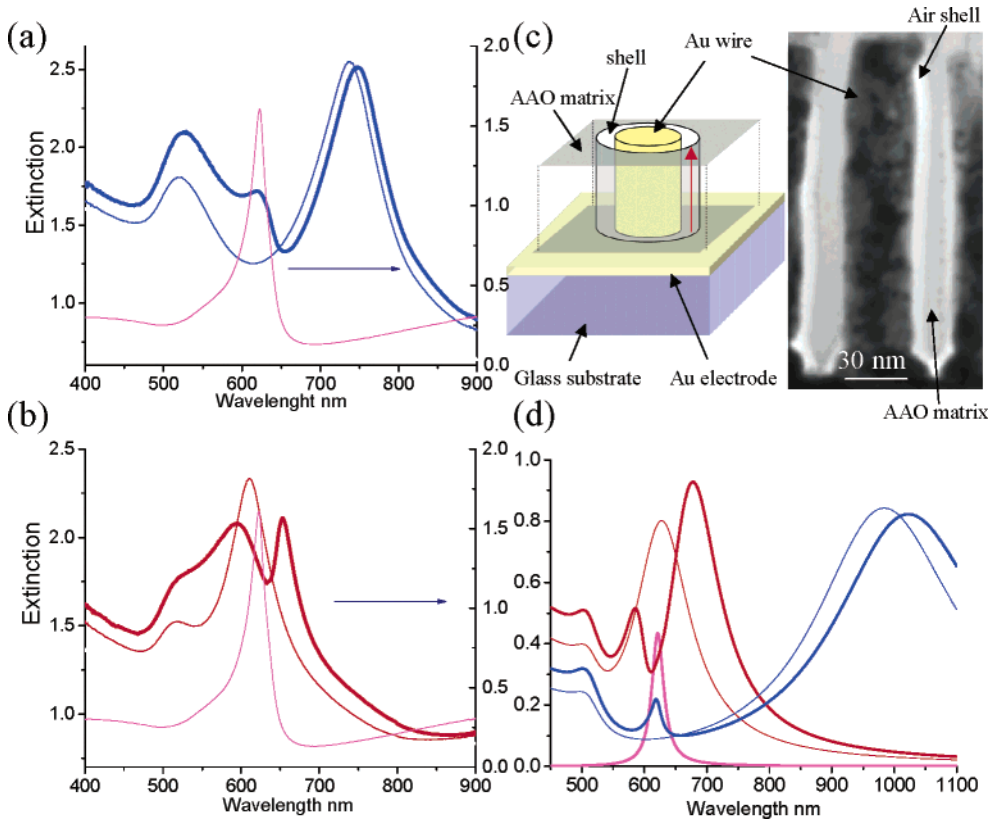

Figure 2. (a) Extinction spectrum of the hybrid ANR in the *weak plasmon−exciton coupling* regime (thick blue line) along with the extinction of the isolated ANR (thin blue line) and the extinction of the J-aggregate on a Au film (magenta line). The shell thickness is 2.5 nm. (b) Extinction spectrum of the hybrid ANR in the *strong plasmon−exciton coupling* regime (thick red line) along with the extinction of the isolated ANR (thin red line) and the extinction of the J-aggregate on a Au film (magenta line). The shell thickness is 20 nm. The spectra are taken for an angle of incidence of 40 degrees. (c) TEM cross section of the ANR core−shell geometry along with a schematic illustration of the structure. The red arrow shows the orientation of the molecular transition dipole moment with respect to the long axis of the Au nanorod when introduced in the shell. (d) Extinction from a coated Au ellipsoid calculated in the dipolar limit and illustrating the general behavior observed experimentally in (a) and (b). Strong and weak coupling regimes are plotted in red and blue colors, respectively. The thin lines correspond to the isolated case, while thick lines describe the response of the hybrid system. A homogeneously broadened J-aggregate extinction is shown in magenta.

between the dipolar long-axis resonance supported by the nanorods when isolated. The latter resonance, which would appear around 2500 nm for an isolated rod of similar aspect ratio, is located in the visible spectral range in the ANR due to inter-rod dipolar coupling. The L-mode collective character is reflected in the associated field distribution that is modified from the long axis dipolar response of isolated rods with maxima around the rods' extremities, to a maximum of the electric field in the inter-rod spacing.[20] Coupling of the excitonic state from the molecular aggregate to either or both the plasmonic modes of the ANR then requires the creation of a shell around the rods in which to introduce the dye.

Recently, we have shown that a simple chemical etching reaction enables the creation of an air−vaccum shell of uniform and tunable thickness around the rods.[21] Such core−shell geometry, illustrated in the TEM picture shown in Figure 2c, opens up unique opportunities to, controllably, couple plasmonic structures with their environment. Indeed, the thickness of the shell represents an additional geometrical parameter, allowing one to tune the optical properties of the plasmonic structure over the 500−900 nm range while simultaneously offering spatial selectivity to couple the plasmonic resonances with active molecules. For this study, shells of various thicknesses were created successively in the same ANR using a 75 mM aqueous solution of sodium hydroxide (NaOH). Etching reactions with 15 s time increments were carried out to create shell thicknesses of 2.5, 3.8, 5.6, 7.7, 8.9, and 20 nm with a thickness distribution, measured by SEM, of 20%. The etching reaction was stopped by rinsing the ANR with purified water (18 MΩ·cm^{-1}). The sample was then dried with pressurized air before hybridization. The hybrid plasmonic−excitonic system was obtained by depositing a 25 μL droplet from a 5% (by weight) benzothiazolium 5-chloro-2-(2-((5-chloro-3-(3-sulfopropyl)-2(3*H*)-benzothiazolylidene)methyl)-1-butenyl)-3-(sulfopropyl), inner salt, compd *N*,*N*-diethylethanamine (1:1) dye (CAS RN 27268-50-4) methanol solution onto the core−shell structure. Upon methanol evaporation, the dye adsorbs onto the Au nanorods within the shell where it spontaneously J-aggregates. Parts a and b of Figure 2 show the extinction of the coupled system for two different shell thicknesses of 2.5 and 20 nm, respectively.[22] The extinction of the J-aggregate when formed on a smooth Au film as well as the extinction of the bare ANR are also plotted in Figure 2a,b for comparison. Varying the shell thickness effectively tunes

the plasmonic resonances of the ANR with no measurable effect on the excitonic transition energy located at a wavelength of 622 nm, approximately. In the following, the shell thickness is therefore used as a parameter to control the spectral overlap between the plasmonic modes of the ANR and the excitonic state of the J-aggregate.

From Figure 2a, it can be deduced that, when the overlap between the L-mode ($\lambda_L = 737$ nm) and the excitonic transition ($\lambda_{JAgg} = 622$ nm) is small, then the spectral response of the extinction associated to the hybrid system ($\lambda_{hybrid+} = 745$ nm, $\lambda_{hybrid-} = 622$ nm) is essentially determined by the resonances of the isolated systems, i.e., *weak coupling* is observed. Conversely, Figure 2b illustrates the regime where this overlap is strong ($\lambda_L = 610$ nm, $\lambda_{JAgg} = 622$ nm). The resonances of the hybrid system ($\lambda_{hybrid+} = 654$ nm and $\lambda_{hybrid-} = 593$ nm) then reflect the *hybridization* of the original resonances into mixed states with shared plasmon−exciton character, i.e., *strong coupling* is observed.

The general behavior observed in Figure 2a,b can be illustrated following the procedure described in ref 13 and calculating the extinction cross section for an isolated ellipsoidal nanoparticles with a Au core surrounded by an excitonic shell and embedded in an homogeneous medium of dielectric constant ϵ_d.[23] This quantity can be expressed as $\sigma_{Extinction_i} = {}^1/_3\sum_i 2\pi/\lambda \mathrm{Im}\{\alpha_i\} + {}^1/_3\sum_i 1/6\pi(2\pi/\lambda)^4|\alpha_i|^2$, where λ is the wavelength in vacuum, and α_i the dipolar polarizability of the core−shell ellipsoid along axis i expressed in the electrostatic approximation.[24] The dielectric constant ϵ_d of the embedding medium alumina is taken to be 2.56, while a polynomial fit of the data published in ref 25 is used to describe the dielectric constant of Au, ϵ_{Au}. The response of the shell was modeled by an excitonic resonance with a Lorentzian response in a dielectric background ϵ_∞. The anisotropy of the exciton's transition dipole moment was approximated by $\epsilon_{JAgg||} = \epsilon_\infty + (\omega_0{}^2 \cdot f)/(\omega_0{}^2 - \omega^2 - i\omega\gamma)$ and $\epsilon_{JAgg\perp} = \epsilon_\infty$ for the contributions along and perpendicular to the aggregate's transition dipole moment, respectively. The high-frequency dielectric constant ϵ_∞ was extracted from ellipsometric measurement made on a thin J-aggregate film formed on a smooth Au surface, while the transition energy, reduced oscillator strength, and damping of the excitonic state were determined by fitting the J-aggregate's absorption spectrum as measured on the smooth Au film in Figure 1b. These parameters then take the respective values of $\epsilon_\infty = 1.21$, $\hbar\omega_0 = 1.99$ eV ($\lambda = 622$ nm), $f = 0.054$, and $\hbar\gamma = 66$ meV. Figure 2d shows the calculated extinction cross section for core−shell ellipsoids with aspect ratios of 2.4 and 6 with a constant shell thickness of 2 nm.[26] The thick lines correspond to the coupled plasmon−exciton system, while the thin lines describe the extinction of the Au ellipsoids but surrounded by an air shell. The extinction of the J-aggregate is also shown alongside by the magenta line spectrum. The aspect ratio of the ellipsoid was parametrized to modify the spectral overlap between the long-axis plasmonic resonance of the ellipsoid and the transition energy of the exciton and, therefore, the coupling strength between the two transition dipole moments.[26] In Figure 2d, only the long-axis plasmonic mode was coupled to the excitonic transition, reflecting the experimental observations. In a situation where both transverse and longitudinal modes from the ellipsoid were to be coupled with the excitonic transition, four modes would be observed in the hybrid's extinction spectrum: two transverse modes as well as two longitudinal modes.

To gain a better insight into the coupling mechanism, let us consider a three-dimensional physical system whose Hamiltonian is H_0. The eigenstates of H_0 are $|\phi_T\rangle$, $|\phi_L\rangle$, and $|\phi_{JAgg}\rangle$ associated to the rod dipolar transverse plasmonic resonance, the ANR's longitudinal resonance, and the J-aggregate excitonic state. The corresponding eigenvalues are E_T, E_L, and E_{JAgg} satisfying $H_0|\phi_T\rangle = E_T|\phi_T\rangle$, $H_0|\phi_L\rangle = E_L|\phi_L\rangle$, and $H_0|\phi_{JAgg}\rangle = E_{JAgg}|\phi_{JAgg}\rangle$, with $\langle\phi_i|\phi_j\rangle = \delta_{ij}$. Introducing coupling between these levels and searching for the eigenvalues of the coupled system in the $\{|\phi_T\rangle, |\phi_L\rangle, |\phi_{JAgg}\rangle\}$ basis, we rewrite the Hamiltonian $H = H_0 + V$, where V is a time-independent perturbation accounting for the coupling between the different eigenstates of the isolated system. Assuming that the J-aggregate's transition dipole moment is oriented along the long axis of the nanorods only, the Hamiltonian takes the following simplified form, where V_{hybrid} couples $|\phi_L\rangle$ and $|\phi_{JAgg}\rangle$:

$$H = \begin{bmatrix} E_T + V_{11} & 0 & 0 \\ 0 & E_L + V_{22} & V_{hybrid} \\ 0 & V_{hybrid} & E_{JAgg} + V_{33} \end{bmatrix} \quad (1.1)$$

from which the eigenvalues are readily obtained:

$$E_T' = E_T + V_{11} \quad (1.2)$$

$$E_{hybrid+} = \frac{1}{2}(E_L' + E_{JAgg}') + \frac{1}{2}\sqrt{(E_L' - E_{JAgg}')^2 + 4V_{hybrid}{}^2} \quad (1.3)$$

$$E_{hybrid-} = \frac{1}{2}(E_L' + E_{JAgg}') - \frac{1}{2}\sqrt{(E_L' - E_{JAgg}')^2 + 4V_{hybrid}{}^2} \quad (1.4)$$

where

$$E_L' = E_L + V_{22} \text{ and } E_{JAgg}' = E_{JAgg} + V_{33}$$

The eigenvector associated with E_T' is $|\psi_T\rangle \sim |\phi_T\rangle$, reflecting the fact that the J-aggregate's transition dipole moment and the T mode were taken to be perpendicular to each other in our expression of the coupling Hamiltonian V. Consequently, for the transverse mode in the hybrid structure, the presence of the J-aggregate along the Au nanorod results in a net change in the energy E_T' through a change in the dielectric constant in the shell, with an eigenvector that is essentially unchanged from its original dipolar form. Neglecting the core−shell geometry as well as the presence of the substrate, an approximate expression for V_{11} can be found by assuming a lossless Drude-like dielectric response of the form $\epsilon(\omega) = 1 - \omega_p^2/\omega^2$ for an Au ellipsoid embedded in an homogeneous medium of effective dielectric constant ϵ_{eff}: $V_{11} = (\hbar\sqrt{L}\omega_p(L - 1))/(2[\epsilon_{eff}(1 - L) + L]^{3/2})\Delta\epsilon_{eff}$, where ω_p is

the bulk plasma frequency of Au, L is the geometric factor defined earlier, and $\Delta\epsilon_{\text{eff}}$ reflects the change in dielectric constant induced by the introduction of the J-aggregate in the shell. V_{11} is an increasing function of the shell thickness through $\Delta\epsilon_{\text{eff}}$ with an upper value of $V_{11} \sim -20$ meV measured for a complete removal of the AAO matrix ($\Delta\epsilon_{\text{eff}} \sim \epsilon_{\text{air}} - \epsilon_{\text{JAgg}\perp} = -0.21$). The negative value of V_{11} reflects the increase index of refraction of the shell when introducing the dye. Similarly to V_{11}, V_{22} reflects the change in the L-mode position upon J-aggregation in the shell via the off-resonance high-frequency dielectric constant of the J-aggregate. However, V_{22} is more difficult to express analytically because the field associated to the L-mode within the ANR is no longer following the dipolar response of the isolated rod's long-axis resonance. An estimated value of V_{22} can be made by measuring the sensitivity of the L-mode as a function of shell thickness for an index of refraction in the shell $\sqrt{\epsilon_{\text{JAgg}\perp}}$ of 1.1.[21] This allows us to evaluate the variation ΔV_{22} of V_{22} over the shell thickness range considered in this study of about 65 meV, while V_{22} at 736 nm is about -20 meV and ΔE_{L} is about 570 meV.[21] V_{33} is a measure of the variation of the intermolecular coupling J within the aggregate when it adsorbs on the Au nanorods with respect to a reference state measured in water: $E_{\text{JAgg}}{}' = E_{\text{JAgg}} + V_{33}$. The loss in potential energy of the highest occupied molecular orbital (HOMO) upon J-aggregation determines the coupling energy J, which can then be defined from the transition energy ΔE_{JAgg} of the aggregate as $2J = \Delta E - \Delta E_{\text{JAgg}}$, where ΔE is the transition energy of the monomer and J is the positive coupling energy. To evaluate V_{33}, J-aggregation has been studied on a smooth Au film, a borosilicate glass substrate, and on porous AAO from the dye solution in methanol. For all those situations, the excitonic transition was observed at an identical wavelength of 622 nm, slightly blue-shifted from its value in water. This underlines that, in the experimental configurations considered, it is the interfacial geometry that governs the aggregation energy rather than the material properties of the substrate itself. Comparing Figure 1b with Figure 2a, it is deduced that J-aggregation in the shell around the rods leads to a intermolecular coupling energy similar to the one measured on planar interfaces, suggesting that the core−shell geometry does not strongly affect the value of J in the aggregate even for the smallest shell thicknesses studied ($\sim$2 nm). Consequently, the value of V_{33} is assumed to be shell-thickness independent in the following. Considering the absorption frequency of the J-aggregate in both water ($\lambda = 650$ nm, i.e., $2J = 230$ meV) and when adsorbed on Au nanorods ($\lambda = 622$ nm, i.e., $2J = 150$ meV), we can deduce that $V_{33} = E_{\text{JAgg}}{}' - E_{\text{JAgg}} = \Delta E - 2J' - (\Delta E - 2J) = 80$ meV.

The eigenvectors $|\psi_+\rangle$ and $|\psi_-\rangle$, associated to respectively $E_{\text{hybrid}+}$ and $E_{\text{hybrid}-}$, can be expressed as linear combinations of the longitudinal plasmonic orbital $|\phi_{\text{L}}\rangle$ and the J-aggregate excitonic orbital $|\phi_{\text{JAgg}}\rangle$ as $|\psi_+\rangle = \cos\alpha/2\ |\phi_{\text{L}}\rangle + \sin\alpha/2\ |\phi_{\text{JAgg}}\rangle$, and $|\psi_-\rangle = -\sin\alpha/2\ |\phi_{\text{L}}\rangle + \cos\alpha/2\ |\phi_{\text{JAgg}}\rangle$, where $\tan\alpha = V_{\text{hybrid}}/(1/2(E'_{\text{L}} - E'_{\text{JAgg}}))$. The effect of the coupling matrix V on H_0 is to hybridize the longitudinal and excitonic states into two new eigenstates with a mixed plasmon−exciton character. It follows that, if $|E'_{\text{L}} - E'_{\text{JAgg}}| \gg 2V_{\text{hybrid}}$, then $\alpha \sim 0$, $\cos\alpha/2 \sim 1$, and $\sin\alpha/2 \sim V_{\text{hybrid}}/|E'_{\text{T}} - E'_{\text{JAgg}}|$, from which, if we assume in this instance that $E'_{\text{L}} > E'_{\text{JAgg}}$, we deduce the wavefunctions of the system as $|\psi_+\rangle = |\phi_{\text{L}}\rangle + (V_{\text{hybrid}}/(E'_{\text{L}} - E'_{\text{JAgg}})\ |\phi_{\text{JAgg}}\rangle \sim |\phi_{\text{L}}\rangle$, and $|\psi_-\rangle = -V_{\text{hybrid}}/(E'_{\text{L}} - E'_{\text{JAgg}})\ |\phi_{\text{L}}\rangle + |\phi_{\text{JAgg}}\rangle \sim |\phi_{\text{JAgg}}\rangle$. These hybrid orbitals then resemble the plasmonic and excitonic orbitals from the uncoupled system, in which case, these orbitals represent a *weakly coupled* system as they retain their original character. This case is illustrated in Figure 2a for $E_{\text{JAgg}}{}' > E_{\text{L}}{}'$. Similarly, if now consider the case for which $|E_{\text{L}}{}' - E_{\text{JAgg}}{}'| \ll 2V_{\text{hybrid}}$, then $\alpha \sim \pi/2$, $\cos\alpha = \sin\alpha \sim 1/\sqrt{2}$, and $|\psi_\pm\rangle = 1/(\sqrt{2})\ [|\phi_{\text{L}}\rangle \pm |\phi_{\text{JAgg}}\rangle]$. These functions are hybrid orbitals of the system of Figure 2b, where the two original uncoupled orbitals overlap spectrally in which case *strong coupling* is achieved.

The unique characteristic of the core−shell ANR geometry is to enable a continuous tuning of the plasmonic resonances by controlling the thickness of the shell created around the rods. The spectral position of the L-mode can therefore be scanned through most of the visible spectrum and across the excitonic resonance to modulate the mixing of these states. The result is shown in Figure 3a, where the spectrum of the hybrid ANR is plotted for different positions of the L-mode in air. The occurrence of the strong coupling regime in the structure is evident because no resonances appear in the spectral range from 622 to 658 nm, while the L-mode resonance was continuously tuned from 736 to 550 nm. The anticrossing between the L-mode and the excitonic transition is illustrated in Figure 3b. Deriving V_{hybrid} from eqs 1.3 and 1.4, we use Figure 3a to estimate the coupling strength within the hybrid as a function of the overlap between the L-mode and the excitonic states as:

$$V_{\text{hybrid}} = \sqrt{\frac{(E_{\text{hybrid}+} - E_{\text{hybrid}-})^2 - (E_{\text{L}} - E'_{\text{JAgg}})^2}{4}} \quad (2)$$

where the assumption $E_{\text{L}}{}' \sim E_{\text{L}}$ was made. The result is plotted in Figure 3c as a function of the original position of the L-mode. A similar relationship derived from an analytical theory for the optical properties of ellipsoidal plasmonic particles covered by anisotropic molecular layers is plotted on top Figure 3c for comparison.[27] These expressions lead to very similar values for V_{hybrid} as a function of the L-mode wavelength with a small overestimation of the coupling strength when using eq 2. This overestimation is reflects the effect V_{22} has on $E_{\text{L}}{}'$: the absolute value of V_{22} increases with shell thickness and is negligible at maximum coupling strength. This maximum is reached for a L-mode resonance in air located at 600 nm and corresponds to a Rabi splitting of 155 meV.[28] This value is commensurate with the largest Rabi splitting observed in planar organic microcavities[29] and similar to recent observations for a excitonic state mixed with a planar SPP.[14]

The ability to control the coupling strength between a plasmon−excitation and a molecular exciton both spatially and spectrally is a major step toward implementing active and passive plasmonic devices. On the basis of the hybrid

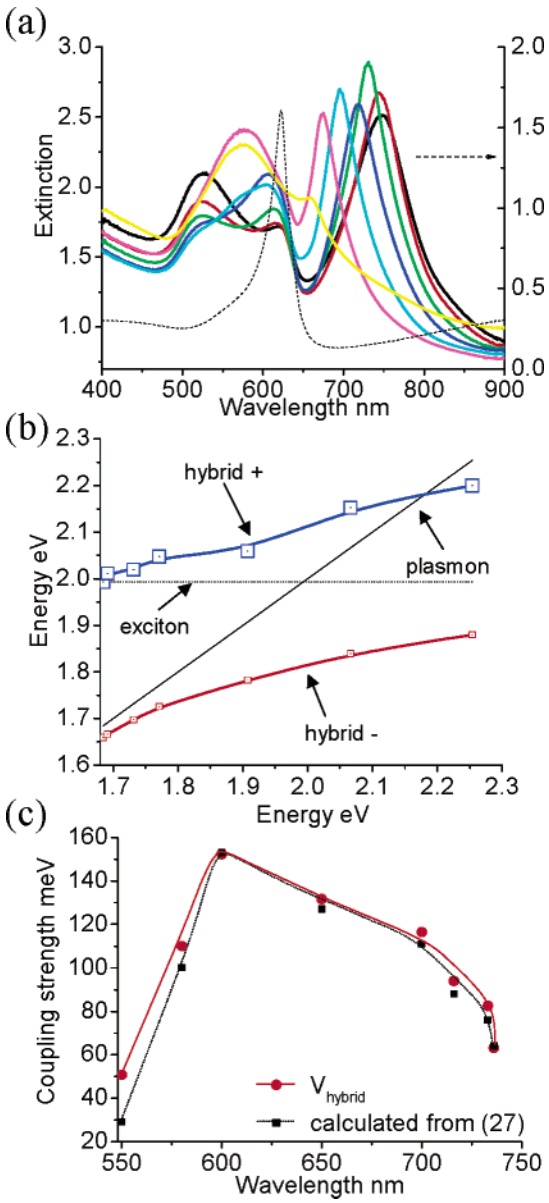

Figure 3. (a) Extinction from the hybrid ANR varying the coupling strength between the plasmonic L-mode and the molecular excitonic transition. The spectra are taken for an angle of incidence of 40°. The plasmon−exciton coupling strength has been adjusted by tuning the spectral position of the L-mode from 736 to 550 nm by increasing the thickness of the shell around the Au rods. The L-mode resonance position in air for the hybrids represented by the black, red, green, blue, cyan, magenta, and yellow spectra was located at a wavelength (and corresponding shell thickness) of 736 nm (2.5 nm), 733 nm (3.8 nm), 716 nm (5.6 nm), 700 nm (7.7 nm), 650 nm (8.9 nm), 600 nm (20 nm), and 550 nm (no shell, matrix completely removed), respectively. The black broken line shows the excitonic extinction on a 50 nm thick smooth Au film. (b) Energy diagram showing the anticrossing of the plasmonic (diagonal solid black line) and the excitonic (horizontal dotted black line). The energy branches of the hybrid system are plotted in red and blue based on (a). The crossing of the high-energy branch and the plasmon line is due to V_{22} upon hybridization (see text for details). The size of the square markers represents the error bars. (c) Coupling strength calculated from eq 2. The data are represented by circular dots, and the red curve is a guide for the eye. For comparison, the black square dots are obtained using the formula for the coupling strength as derived in ref 27. The dotted line is a guide for the eye.

nature of the coupled states, the nonlinear optical properties of such a nanostructured material should demonstrate extreme sensitivity over a large spectral range, i.e., by addressing one of the hybrid resonances, one would effectively affect both coupled resonances and therefore affect the extinction of the device from 550 to 700 nm. This could be achieved optically in a pump−probe configuration, for example, and possibly also electrically by dynamically controlling the orientation/ordering of the molecular aggregate. Because of the coupled nature of the resonances, future investigations on the emission properties of this hybrid structure are of considerable interest as well.[14] Finally, we emphasize the practical interest of such device, as the ANR's fabrication process is simple and scalable[21] while also demonstrating strong potential in the fabrication of nanodevices.[30]

Acknowledgment. This work was supported, in part, by EPSRC (UK) and EU FP6 Network of Excellence Plasmo-Nano-Devices. The authors are grateful to Invest Northern Ireland for the provision of funding under Nanotec NI, facilitating the formation of the Centre for Nanostructured Media at the Queen's University of Belfast.

References

(1) Barnes, W. L.; Dereux, A.; Ebbesen, T. W. *Nature* **2003**, *424*, 824.
(2) Andrew, P.; Barnes, W. L. *Science* **2004**, *306*, 1002.
(3) Zayats, A. V.; Smolyaninov, I. I.; Maradudin, A. A. *Phys. Rep.* **2005**, *408*, 131.
(4) Raether, H. *Surface Plasmons on Smooth and Rough Surfaces and on Gratings*; Springer: New York, 1987; Vol. 111.
(5) Laurent, G.; Felidj, N.; Grand, J.; Aubard, J.; Levi, G.; Hohenau, A.; Aussenegg, F. R.; Krenn, J. R. *Phys. Rev. B* **2006**, *73*, 245417.
(6) McFarland, A. D.; Duyne, R. P. V. *Nano Lett.* **2003**, *3*, 1057.
(7) Maier, S. A.; Atwater, H. A. *J. Appl. Phys.* **2005**, *98*, 011101.
(8) Haes, A. J.; Zou, S.; Zhao, J.; Schatz, G. C.; VanDuyne, R. P. *J. Am. Chem. Soc.* **2006**, *128*, 10905.
(9) Seidel, J.; Grafstrom, S.; Eng, L. *Phys. Rev. Lett.* **2005**, *94*, 177401.
(10) Wurtz, G. A.; Pollard, R.; Zayats, A. V. *Phys. Rev. Lett.* **2006**, *97*, 057402.
(11) Kobayashi, T. *J-Aggregates*; World Scientific: Singapore, 1996.
(12) Ozcelik, S.; Ozcelik, I.; Akins, D. L. *Appl. Phys. Lett.* **1998**, *73*, 1949.
(13) Wiederrecht, G. P.; Wurtz, G. A.; Hranisavljevic, J. *Nano Lett.* **2004**, *4*, 2121.
(14) Bellessa, J.; Bonnand, C.; Plenet, J. C.; Mugnier, J. *Phys. Rev. Lett.* **2004**, *93*, 036404.
(15) Dintinger, J., S. K.; Bustos, F.; Barnes, W. L.; Ebbesen, T. W. *Phys. Rev. B* **2005**, *71*, 035424.
(16) Lidzey, D. G.; Bradley, D. D. C.; Armitage, A.; Walker, S.; Skolnick, M. S. *Science* **2000**, *288*, 1620.
(17) Hobson, P. A.; Barnes, W. L.; Lidzey, D. G.; Gehring, G. A.; Whittaker, D. M.; Skolnick, M. S.; Walker, S. *Appl. Phys. Lett.* **2002**, *81*, 3519.
(18) Christ, A.; Tikhodeev, S. G.; Gippius, N. A.; Kuhl, J.; Giessen, H. *Phys. Rev. Lett.* **2003**, *91*, 183901.
(19) Atkinson, R.; Hendren, W. R.; Wurtz, G. A.; Dickson, W.; Zayats, A. V.; Evans, P.; Pollard, R. J. *Phys. Rev. B* **2006**, *73*, 235402.
(20) Wurtz, G. A.; Dickson, W.; Atkinson, R.; Hendren, W.; Evans, P.; Pollard, R.; Zayats, A. V. **2006**, submitted for publication.
(21) Evans, P. R.; Wurtz, G. A.; Atkinson, R.; Hendren, W.; Dickson, W.; Pollard, R. J.; Zayats, A. V. **2006**, submitted for publication.
(22) Additional experiments established that the response of the exciton from the aggregate formed at the ANR's top interface represent a negligible contribution to the overall extinction.
(23) Similar results are obtained using the model presented in ref 27 accounting for inter-rod interactions within the ANR. However, our motivation here is to illustrate the generality of the experimental observation by using the most simplistic model.
(24) Bohren, C. F.; Huffmann, D. R. *Absorption and Scattering of Light by Small Particles*; Wiley Science: New York, 1983.

(25) Johnson, P. B.; Christy, R. W. *Phys. Rev. B* **1972**, *6*, 4370.
(26) Neglecting inter-rod interactions in the model calculations leads to discrepancies in the rod's aspect ratio between the values used in the calculations and the experimental aspect ratio of 16.
(27) Ambjörnsson, T.; Mukhopadhyay, G.; Apell, S. P.; Käll, M. *Phys. Rev. B* **2006**, *73*, 085412.
(28) Note that the coupling strength is plotted as a function of the L-mode resonance position in air, i.e., without accounting for the red-shift of this resonance induced by V_{22} when the aggregate is formed around the rods.
(29) Agranovich, V. M.; Litinskaia, M.; Lidzey, D. G. *Phys. Rev. B* **2003**, *67*, 085311.
(30) Vlad, A.; Matefi-Tempfli, M.; Faniel, S.; Bayot, V.; Melinte, S.; Piraux, L.; Matefi-Tempfli, S. *Nanotechnology* **2006**, *17*, 4873.

NL070284M